

## EVOLUTION OF THE *K*-BAND GALAXY CLUSTER LUMINOSITY FUNCTION AND SCALING RELATIONS

YEN-TING LIN<sup>1,2,3</sup>, JOSEPH J. MOHR<sup>1,2,4</sup>, ANTHONY H. GONZALEZ<sup>1,5</sup>, AND S. ADAM STANFORD<sup>1,6</sup>

*ApJL, accepted*

### ABSTRACT

We study the evolution of two fundamental properties of galaxy clusters: the luminosity function (LF) and the scaling relations between the total galaxy number  $N$  (or luminosity) and cluster mass  $M$ . Using a sample of 27 clusters ( $0 \leq z \leq 0.9$ ) with new near-IR observations and mass estimates derived from X-ray temperatures, in conjunction with data from the literature, we construct the largest sample for such studies to date. The evolution of the characteristic luminosity of the LF can be described by a passively evolving population formed in a single burst at  $z = 1.5 - 2$ . Under the assumption that the mass-temperature relation evolves self-similarly, and after the passive evolution is accounted for, the  $N$ - $M$  scaling shows no signs of evolution out to  $z = 0.9$ . Our data provide direct constraints on halo occupation distribution models, and suggest that the way galaxies populate cluster-scale dark matter halos has not changed in the past 7 Gyr, in line with previous investigations.

*Subject headings:* cosmology: observation – galaxies: clusters: general – galaxies: luminosity function, mass function – galaxies: formation – infrared: galaxies

### 1. INTRODUCTION

The subject of cluster galaxy evolution has always been central to cluster studies. For the early types that comprise the majority of the cluster galaxies, studies based on the fundamental plane and/or color-magnitude relations suggest that their stars are primarily old, and evolve passively with time (e.g. Bower et al. 1992; Stanford et al. 1998; Kelson et al. 2000). Given the hierarchical nature of structure formation, changes in the galaxy population over cosmic time are expected. Numerous investigations have reported such evidence, e.g. a higher fraction of blue galaxies in more distant clusters (e.g. Butcher & Oemler 1978; Ellingson et al. 2001), a decline in the S0 galaxy abundances towards higher- $z$  (Dressler et al. 1997), and a population that appears to be in the post-starburst phase (Poggianti et al. 1999).

A powerful method for quantifying galaxy populations is via the luminosity function (LF). The characteristic luminosity of the cluster galaxies as a whole is reflected by the “knee” of the LF ( $M_*$ ); comparison of LFs at different redshifts thus will indicate the evolution of the mean galaxy population and constrain the formation epoch of cluster galaxies (e.g. Barger et al. 1998; De Propriis et al. 1999; Strazzullo et al. 2006).

Here we present an analysis of the evolution of the cluster  $K_s$ -band LF from  $z = 0$  to  $z = 0.9$ , which has several novelties and advantages over previous studies. Foremost, all our clusters have mass estimates accurate to  $\lesssim 30\%$  (from the X-ray temperature  $T_X$ ). We construct the LF within the same portion of the cluster virial radius, which facilitates comparisons of clusters at different redshifts and of different masses. We also make use of the cluster mass information and construct the LF in terms of space density. Finally, our data generally are deeper, and cover a larger fraction of the cluster virial region.

These aspects allow us to integrate the LF to estimate the total galaxy luminosity ( $L$ ) and number ( $N$ ), and study their correlation with the cluster mass ( $M$ ). Based on a large sample of nearby clusters, we have found tight correlations between  $L$  or  $N$  with  $M$  (Lin et al. 2003, 2004, hereafter L03, L04, respectively), which already provide an interesting constraint on the regularity of the cluster galaxy formation process.

In this study we pay special attention to the evolution of the  $N$ - $M$  relation, which directly constrains simple clustering models such as the halo occupation distribution (HOD; e.g. Berlind & Weinberg 2002) out to  $z \sim 1$ . In such models, the way galaxies populate dark matter halos (e.g. the number of cluster galaxies above some luminosity limit as a function of halo mass, known as the halo occupation number) are tuned until the observed galaxy clustering at both small and large scales is reproduced. Physics of galaxy formation is studied by identifying mechanisms that reproduce the halo occupation statistics (e.g. Zheng et al. 2005). Furthermore, the evolution of the  $N$ - $M$  relation may reveal the mass function evolution of subhalos in cluster-size halos (Cooray & Milosavljević 2005).

In §2 we describe the sample selection, observations, data reduction, and our methods for the star-galaxy separation. We stack the cluster data to construct the composite LFs at different redshifts (§3), which enable us to constrain the evolution of  $M_*$  and the formation epoch of the cluster galaxies. We then proceed to solve for the LF parameters of individual clusters, and examine the evolution of the  $L$ - $M$  and  $N$ - $M$  relations (§4). We discuss our main findings in §5. We assume the cosmological parameters to be  $(\Omega_M, \Omega_\Lambda, H_0) = (0.3, 0.7, 70 h_{70} \text{ km s}^{-1} \text{ Mpc}^{-1})$ . Throughout the paper we denote  $K_s$ -band by  $K$ -band for brevity, and adopt the Vega magnitudes unless noted ( $K_{AB} - K_{\text{Vega}} = 1.85$ , Blanton & Roweis 2006).

### 2. THE DATA

The cluster sample used here is drawn from several catalogs, and the selection is heterogeneous. All our clusters have measured  $T_X$ , and have been observed by either *Chandra* or *XMM*. The cluster near-IR (NIR) data were acquired with *FLAMINGOS* (hereafter FLMN) over several observing runs at the KPNO 4m and 2.1m telescopes, generally under  $1.1'' - 1.5''$  seeing. Some of the basic information for the 27 clusters in our sample is listed in Table 1, including: the clus-

<sup>1</sup> Visiting Astronomer, KPNO, NOAO.

<sup>2</sup> Department of Astronomy, University of Illinois, Urbana, IL 61801

<sup>3</sup> Current Address: Departamento de Astronomía y Astrofísica, Pontificia Universidad Católica de Chile; Princeton University Observatory, Princeton University, Princeton, NJ 08544; ytlin@astro.princeton.edu

<sup>4</sup> Department of Physics, University of Illinois, Urbana, IL 61801

<sup>5</sup> Department of Astronomy, University of Florida, Gainesville, FL 32611

<sup>6</sup> Department of Physics, University of California, Davis, CA 95616; IGGP, LLNL, Livermore, CA 94551

TABLE 1  
THE CLUSTER DATA

Name	$z$	$T_X$	$K_{lim}$	$\theta_{max}/\theta_{200}$	Remarks <sup>a</sup>
Abell2052	0.0355	3.4	19.3	0.35	2m,S
Abell0085	0.0551	6.1	18.8	0.39	2m,S
Abell1795	0.0625	5.5	19.0	0.47	2m,S
Abell2029	0.0773	9.1	19.0	0.44	2m,S
Abell2255	0.0806	6.87	18.3	0.53	2m,S
Abell2142	0.0909	8.46	18.7	0.54	2m,S
Abell2244	0.0968	7.1	18.6	0.62	2m,S
Abell2055	0.1020	5.8	19.3	0.73	2m,S
Abell2034	0.1130	7.93	18.8	0.68	2m,S
Abell1413	0.1430	6.56	19.0	0.89	2m,S
Abell1204	0.1710	3.58	18.9	0.92	2m,S
Abell1914	0.1712	8.41	18.4	0.97	2m,S
Abell1689	0.1832	8.58	19.3	1.02	2m,S
Abell2390	0.228	11.5	19.3	0.50	4m,J
RXJ129.7+0005	0.234	6.78	19.4	0.68	4m,J,S
Abell1835	0.2532	9.5	19.3	0.61	4m,J,S
Abell1758	0.279	6.57	18.6	1.70	2m,J,S
Abell1995	0.319	10.37	19.6	0.72	4m,J,S
MS1358.4+6245	0.328	6.92	20.4	0.91	4m,J,S
MS1621.5+2640	0.426	7.6	20.0	1.09	4m,J,S
RXJ1347.5-1145	0.451	14.1	18.8	0.83	4m,J
RXJ1701.3+6414	0.453	5.8	18.7	1.33	4m,S
RXJ1524.6+0957	0.516	5.1	19.8	1.59	4m,S
MACS0717.5+3745	0.548	14.4	19.3	0.97	4m,J
MACS0647.7+7015	0.584	11.58	19.0	1.16	4m,J
RXJ1120.1+4318	0.6	5.3	20.0	1.79	4m,J,S
MACS0744.8+3927	0.686	10.04	19.3	1.44	4m,J,S

<sup>a</sup>2m & 4m indicate the KPNO telescope used; J means  $J$ -band data also available; S means the cluster is covered by SDSS DR5.

ter name, the redshift and  $T_X$  (in keV) of the cluster, the limiting  $K$ -band magnitude, the fraction of the cluster virial radius  $r_{200}$ <sup>7</sup> that the FLMN field-of-view (FOV) corresponds to, and the available data in other bands ( $J$  and optical bands from the SDSS). The reduction of the data was carried out by a pipeline developed at the University of Florida (see Elston et al. 2006).

To increase the coverage in both redshift and mass, we supplement our FLMN data with those presented in Stanford et al. (2002, hereafter S02). The 45 clusters in S02 were not selected by any well-defined criteria, and the data were obtained with several different telescopes and instruments. These instruments have a much smaller FOV than FLMN. Some of these data have been used by De Propriis et al. (1999, hereafter DP99) for the study of the  $K$ -band LF evolution. We include 14 clusters from S02 that have measured  $T_X$  and both  $J$  and  $K$ -band data. The combined sample includes 41 clusters from  $z \sim 0$  to  $z \approx 0.9$ , all of which are observed out to at least  $r_{2000} \approx r_{200}/3$  (Table 1).

The varying point spread function across the FLMN array prevents the use of morphological information for star-galaxy separation from our images. For the majority of clusters at  $z \geq 0.2$ , both  $J$  and  $K$ -band photometry are available. In this case  $J-K > 1$  can be used to select galaxies from the source catalog (DP99). For the clusters that lack  $J$ -band data, we use data from the SDSS for help in star-galaxy separation. Objects identified by the SDSS as point sources with  $i_{AB} \leq 21.3$

<sup>7</sup> The virial mass is inferred from  $T_X$  using the empirical mass-temperature relation obtained by Finoguenov et al. (2001). Self-similar evolution of the relation is assumed. We denote the radius within which the mean overdensity is  $\Delta$  times the critical density as  $r_{\Delta}$ . The Navarro et al. (1997, NFW) profile with concentration  $c = 5$  is used for converting between radii of different overdensities (e.g.  $r_{700} = 0.56r_{200}$ ,  $r_{1000} = 0.47r_{200}$ ,  $r_{2000} = 0.33r_{200}$ ). We use a  $c = 3$  profile for the spatial distribution of galaxies within clusters (L04).

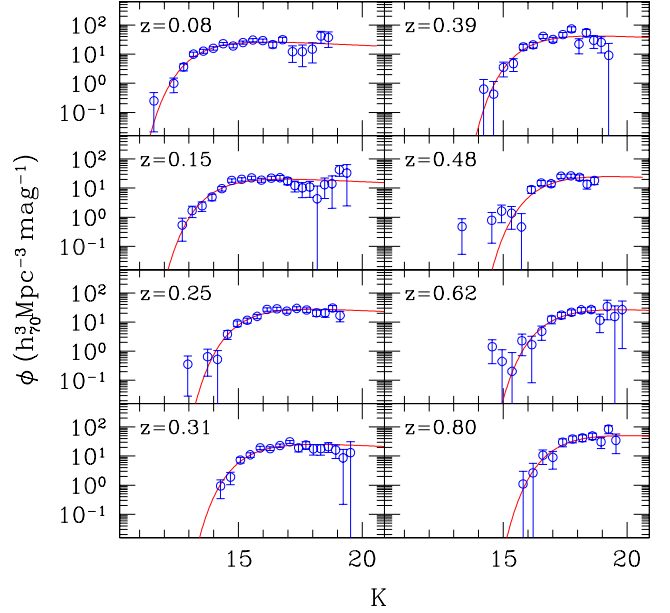


FIG. 1.— The evolution of apparent LFs, evaluated within  $r_{2000}$ . The LFs are presented in terms of the *physical* space density (as opposed to the comoving density). The binning in redshift, and the number of clusters in each bin are:  $0 \leq z < 0.1$  (7),  $0.1 \leq z < 0.2$  (6),  $0.2 \leq z < 0.3$  (4),  $0.3 \leq z < 0.34$  (8),  $0.34 \leq z < 0.45$  (4),  $0.45 \leq z < 0.55$  (3),  $0.55 \leq z < 0.7$  (4),  $0.7 \leq z < 0.9$  (5). The midpoint redshifts are marked in each panel.

(the 95% completeness limit for point sources) are regarded as stars. Based on the  $i-K$  color distribution of the sources from the FLAMINGOS Extragalactic Survey (Elston et al. 2006, hereafter FLAMEX), we find that for objects brighter than  $K = 18.06$ , the SDSS identifies 95% of the stars. For objects fainter than  $i_{AB} = 21.3$ , we filter out the stars with the criterion  $(g-i)_{AB} \geq 1.4(i-K)_{AB} + 0.99$ , which is a cut that we determine will filter 90% of the stars. At  $K > 18.06$  the galaxy surface density outnumbers that of the stars, and we conclude that our star-galaxy separation scheme will induce  $< 1\%$  contamination in the final galaxy catalogs.

### 3. $K$ -BAND LUMINOSITY FUNCTIONS FROM $z = 0$ TO $z = 0.9$

The method developed in L03 for obtaining the total galaxy luminosity or number of a cluster is to use the observed, background-corrected galaxy number and flux to solve for the LF parameters  $M_*$  and  $\phi_*$ , assuming a fixed faint-end power-law slope  $\alpha$  of the LF. Before we study the  $N-M$  and  $L-M$  relations at intermediate redshifts, it is important to examine the evolution of the LF, as this (1) allows us to understand the behavior of the faint-end, and (2) provides a means to apply the evolution correction to the observed galaxy flux.

Using the number counts derived from the FLAMEX survey for statistical background correction, we follow L04 to construct the composite LF in the observer's frame in eight redshift bins (Fig. 1). For each bin, we choose a midpoint redshift  $z_{cen}$ , and adjust the  $k$ -correction and distance modulus of individual clusters to best represent how the clusters would appear if they were all at  $z_{cen}$  (e.g. DP99). The combined corrections are typically less than  $\pm 0.3$  mag. As we discuss in L04, the main difference in the LFs between high and low mass clusters is the normalization  $\phi_*$ . Because our purpose here is to examine the evolution of the LF shape, we ignore this difference in constructing the composite LF. In each panel

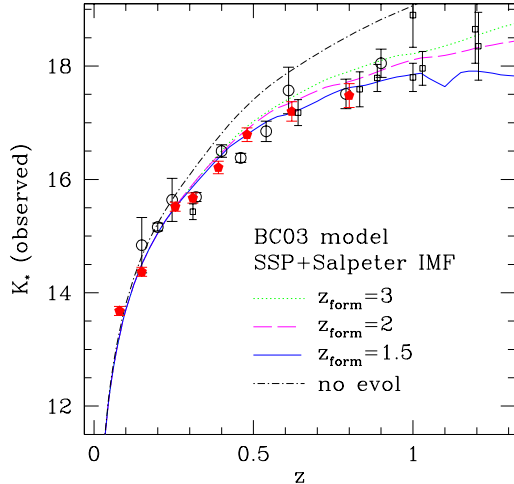


FIG. 2.— Evolution of  $K_*$  as determined within  $r_{2000}$  (solid pentagons). Results from DP99 are shown as hollow circles. Other data points (open squares) are: two clusters at  $z = 0.31$  (Andreon et al. 2005), EIS0048 at  $z = 0.64$  (Massarotti et al. 2003), three clusters at  $z = 0.83, 0.89,$  and  $1.03$  (Ellis & Jones 2004), two clusters at  $z \sim 1$  (Kodama & Bower 2003), MG2016+112 at  $z = 1$  (Toft et al. 2003), cluster 3C324 at  $z = 1.2$  (Nakata et al. 2001), and three clusters at  $z = 1.2$  (Strazzullo et al. 2006).

we show the best-fit Schechter (1976) function to the data, with  $\alpha = -0.9$ . This value is consistent with what we find in L04, and has been adopted by several previous studies. We also note that the shape of the LFs ( $K_*$  and the faint-end) does not change significantly within 30–60% of  $r_{200}$ , which means the LFs shown in the Figure (evaluated within  $r_{2000}$ ) should be representative of the LF evolution.

In Fig. 2 we show the best-fit  $K_*$  as a function of redshift, and compare them with the predictions from a population synthesis model (Bruzual & Charlot 2003, hereafter BC03). The model galaxies are formed with the Salpeter initial mass function and solar metallicity in a single burst at  $z_{\text{form}} = 1.5, 2,$  and  $3$ . We have normalized the model predictions to the  $M_*$  found in L04. The dot-dashed line in the Figure shows the  $K_*$  with no evolution correction applied. We also show the results from several previous studies, mainly that of DP99. Our data, together with most of the clusters at  $z \leq 1$  from the literature, seem to favor the model where the stars in clusters are formed at  $z_{\text{form}} = 1.5-2$ . None of the previous studies noted here examines the LF at a fixed fraction of the virial radius. In the absence of any radial dependence of the  $M_*$  (see e.g. L04), studying a region that is a constant fraction of the virial region is not required. Because we look at the cluster galaxies as a whole, the behavior of  $K_*(z)$  would also reflect the evolution of field galaxies that fall into clusters much later than the old spheroids. Our inferred  $z_{\text{form}}$  therefore seems low compared to that derived from studies targeting early type cluster galaxies (e.g. Ellis et al. 1997).

#### 4. EVOLUTION OF THE NEAR-IR SCALING RELATIONS

The results from the previous section indicate that (1) a passively evolving stellar population formed in a single burst at  $z = 1.5$  can describe the LF (of the whole cluster galaxy population) evolution based on our  $z < 0.9$  cluster sample, and (2) the faint-end slope of LFs is consistent with  $\alpha = -0.9$  at all redshifts. We can then use the BC03 model prediction of the spectral aging for the  $k$ - and evolution corrections. We follow L03 to obtain the total galaxy luminosity and number for

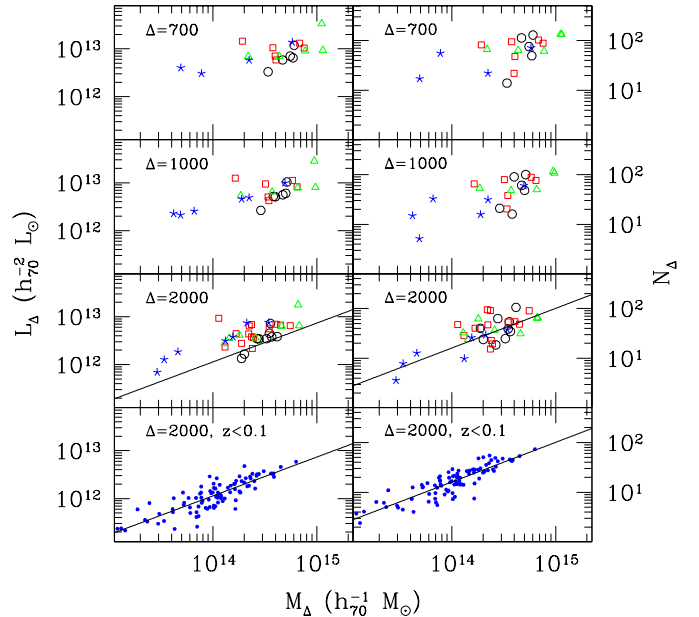


FIG. 3.— The panels on the left (right) column show the  $L-M$  ( $N-M$ ) correlation. The top three rows are the results measured within  $r_{700}, r_{1000},$  and  $r_{2000}$ , respectively. Clusters in each redshift bin are plotted with different styles:  $z = 0.0-0.2$ : circle;  $z = 0.2-0.4$ : square;  $z = 0.4-0.6$ : triangle;  $z = 0.6-0.9$ : star. The bottom row shows the correlations for the  $z < 0.1$  local cluster sample (see text for details). The straight lines in the bottom two rows show the best-fit  $L-M$  and  $N-M$  correlations for the local sample.

our clusters. Specifically, we integrate the LF over all galaxies more luminous than  $M_{K_*}(z) + 2$ , where  $M_{K_*}(z)$  is the restframe characteristic magnitude based on the BC03 model.

We show in Fig. 3 the  $L-M$  and  $N-M$  correlations evaluated within  $r_{700}, r_{1000},$  and  $r_{2000}$ . Clusters are binned into four redshift bins. It is interesting to see that these correlations also exist for the intermediate redshift clusters studied here. For comparison, in the bottom panels are shown the correlations for the 93 clusters at  $z < 0.1$  studied by L04 (hereafter the local sample). For these local clusters  $L$  and  $N$  are both first determined within  $r_{200}$  [down to  $M_{K_*}(z = 0) + 2$ ], then scaled to  $r_{2000}$  using an NFW profile with  $c = 3$  (e.g. L04).

We examine the existence and the form of evolution in the data by considering

$$N(M, z) = N_0(1+z)^\gamma (M/M_0)^s \quad (1)$$

for the  $N-M$  evolution, where  $N_0$  and  $M_0$  are the normalization factors of the relation. The evolution is specified by  $\gamma$ . With  $M_0$  set at  $10^{14.3} M_\odot$ , we fit the above expression to all clusters to find out the parameters ( $N_0, \gamma, s$ ). It is expected that the parameters  $\gamma$  and  $s$  would exhibit some degeneracy, and therefore we also include the local sample for this exercise, whose size and the range in mass would greatly help determine  $N_0$  and  $s$ . Within different regions (e.g.  $r_{700}, r_{1000},$  and  $r_{2000}$ ), the constraints on the evolution of the  $N-M$  relation are consistent. For simplicity, we only present the results from  $N_{2000}-M_{2000}$  correlations, which are the tightest of the three cases. In Fig. 4 we show the joint constraints for  $\gamma$  and  $s$ . The smaller (larger) contour is obtained when the local sample is included (excluded). The contours correspond to 68% confidence region. For each case the best-fit ( $\gamma, s$ ) is shown as the symbol at the center of the contour. Combining both samples results in a much tighter constraint on

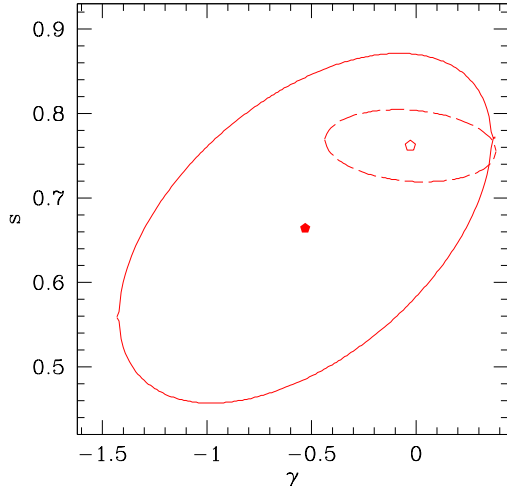


FIG. 4.— Joint 68% confidence region for  $\gamma$  and  $s$  (see Eqn. 1 for the definition). The large contour results when Eqn. 1 is fit to the high- $z$  sample. A tighter constraint on  $\gamma$  is obtained when both high- $z$  and local samples are used (the dashed contour). The points show the best-fit values for  $(\gamma, s)$ :  $(-0.53, 0.66)$  for the high- $z$  sample, and  $(-0.03, 0.76)$  for the combined sample.

$\gamma$ . If we further marginalize over  $s$ , we find that without the local sample,  $\gamma = -0.53 \pm 0.59$ ; inclusion of the local sample gives  $\gamma = -0.03 \pm 0.27$ . Both results are consistent with a no-evolution scenario.

## 5. DISCUSSION

We can understand the no-evolution of the  $N$ – $M$  relation by looking at the integration of the LF:

$$N(M, z) = V \phi_* \Gamma(\alpha + 1, L_l(z)/L_*(z)), \quad (2)$$

where  $V$  is the cluster volume,  $L_l$  is the luminosity corresponding to the lower limit of the integration, and  $\Gamma$  is the incomplete gamma function. Because  $L_l$  is set to be a fixed fraction of  $L_*$ , it is the product of  $V$  and  $\phi_*$  that determines  $N$ . For two clusters  $i$  and  $j$  which have the same mass but at different redshifts (say  $z_j > z_i$ ),  $V_j < V_i$  (assuming that  $r_\Delta \propto 1/H(z)$ , where  $H(z)$  is the expansion rate of the Universe). One thus expects that on average,  $\phi_{*j} > \phi_{*i}$ . Indeed,  $\phi_*$  derived for our clusters agrees with this expectation. *That the increase in the galaxy number density is offset by the decrease in the virial volume is the main reason for the lack of evolution of the  $N$ – $M$  relation.*

Previous studies have found suggestions of lack of HOD evolution toward  $z \sim 1$ , based on clustering statistics (Yan et al. 2003; Phleps et al. 2006; Coil et al. 2006). In a recent attempt to extract both cosmological information and cluster physics from a large sample of clusters, it is found that the optical observable–mass relation, although only weakly constrained, does not evolve with redshift (Gladders et al. 2006). We note, however, passive evolution has not been accounted for in this analysis (S. Majumdar 2006, private communication). Our study is complementary in the sense that we probe the (high mass end of) occupation number directly, with reliable cluster mass estimates from  $T_X$ .

It is possible that changes in both the red and blue galaxy populations with redshift are hidden from the evolution of the  $N$ – $M$  relation, if they conspire to make the total galaxy number unchanged. We are in the process of acquiring color information in order to constrain the evolution of these populations separately.

The fact that only when the large, nearby cluster sample of L04 is included can we obtain reasonably tight constraint on the  $N$ – $M$  evolution points to the need for a *much* larger sample with reliable mass estimates at higher- $z$ . This is also demanded for large optical/NIR cluster surveys which may rely on optical/NIR based cluster mass estimators (e.g. FLAMEX). Based on simple Monte Carlo simulations, we estimate that at least 20 clusters at  $z = 0.8$ – $1.0$  are required to constrain  $\gamma$  to 0.1 level. While more clusters at intermediate redshifts may provide better constraints on the evolution of the slope of the scaling relation,  $z > 1$  clusters clearly will help pinpoint the formation epoch of the cluster galaxies.

This paper is dedicated to the memory of Richard Elston, whose instrument, *FLAMINGOS*, and observation programs, are essential to this analysis. We acknowledge Z. Zheng, A. Sanderson, D. Nagai, and D. Stern for useful comments on the manuscript. D. Stern is also thanked for help in data acquisition. We thank an anonymous referee for helpful suggestions. JJM and YTL acknowledge support from NSF OPP award OPP-0130612 and NASA LTSA award NAG5-11415. YTL is also supported by NSF PIRE grant OISE-0530095. AHG acknowledges support from NSF award AST-0436681. SAS's work was performed under the auspices of the U.S. DOE, NNSA by the UC, LLNL under contract No. W-7405-Eng-48. This work uses data acquired as part of the FLAMEX program. This publication has made use of data products from the SDSS. Its website is <http://www.sdss.org/>.

## REFERENCES

- Andreon, S., Punzi, G., & Grado, A. 2005, MNRAS, 360, 727  
 Barger, A. J., et al. 1998, ApJ, 501, 522  
 Berlind, A. A. & Weinberg, D. H. 2002, ApJ, 575, 587  
 Blanton, M. R. & Roweis, S. 2006, AJ, submitted (astro-ph/0606170)  
 Bower, R. G., Lucey, J. R., & Ellis, R. S. 1992, MNRAS, 254, 601  
 Bruzual, G. & Charlot, S. 2003, MNRAS, 344, 1000 (BC03)  
 Butcher, H. & Oemler, A. 1978, ApJ, 219, 18  
 Coil, A. L., et al. 2006, ApJ, 638, 668  
 Cooray, A. & Milosavljević, M. 2005, ApJ, 627, L89  
 De Propris, R., Stanford, S. A., Eisenhardt, P. R., Dickinson, M., & Elston, R. 1999, AJ, 118, 719 (DP99)  
 Dressler, A., et al. 1997, ApJ, 490, 577  
 Ellingson, E., Lin, H., Yee, H. K. C., & Carlberg, R. G. 2001, ApJ, 547, 609  
 Ellis, R. S., Smail, I., Dressler, A., Couch, W. J., Oemler, A. J., Butcher, H., & Sharples, R. M. 1997, ApJ, 483, 582  
 Ellis, S. C. & Jones, L. R. 2004, MNRAS, 348, 165  
 Elston, R. J., Gonzalez, A. H., et al. 2006, ApJ, 639, 816  
 Finoguenov, A., Reiprich, T. H., & Böhringer, H. 2001, A&A, 368, 749  
 Gladders, M. D., Yee, H. K. C., Majumdar, S., Barrientos, L. F., Hoekstra, H., Hall, P. B., & Infante, L. 2006, ApJ, submitted (astro-ph/0603588)  
 Kelson, D. D., Illingworth, G. D., van Dokkum, P. G., & Franx, M. 2000, ApJ, 531, 184  
 Kodama, T. & Bower, R. 2003, MNRAS, 346, 1  
 Lin, Y.-T., Mohr, J. J., & Stanford, S. A. 2003, ApJ, 591, 749 (L03)  
 —. 2004, ApJ, 610, 745 (L04)  
 Massarotti, M., Busarello, G., La Barbera, F., & Merluzzi, P. 2003, A&A, 404, 75  
 Nakata, F., et al. 2001, PASJ, 53, 1139  
 Navarro, J. F., Frenk, C. S., & White, S. D. M. 1997, ApJ, 490, 493  
 Phleps, S., Peacock, J. A., Meisenheimer, K., & Wolf, C. 2006, A&A, accepted (astro-ph/0506320)  
 Poggianti, B. M., Smail, I., Dressler, A., Couch, W. J., Barger, A. J., Butcher, H., Ellis, R. S., & Oemler, A. J. 1999, ApJ, 518, 576  
 Schechter, P. L. 1976, ApJ, 203, 297  
 Stanford, S. A., Eisenhardt, P. R., & Dickinson, M. 1998, ApJ, 492, 461  
 Stanford, S. A., Eisenhardt, P. R., Dickinson, M., Holden, B. P., & De Propris, R. 2002, ApJS, 142, 153

Strazzullo, V., et al. 2006, *A&A*, 450, 909

Toft, S., Soucail, G., & Hjorth, J. 2003, *MNRAS*, 344, 337

Yan, R., Madgwick, D. S., & White, M. 2003, *ApJ*, 598, 848

Zheng, Z., et al. 2005, *ApJ*, 633, 791